Solar Cosmic Rays of February, 1956 and Their Propagation through Interplanetary Space*

P. MEYER, E. N. PARKER, AND J. A. SIMPSON
Enrico Fermi Institute for Nuclear Studies, The University of Chicago, Chicago, Illinois
(Received July 2, 1956)

The data from six neutron-intensity monitors distributed over a wide range of geomagnetic latitudes have been used to study the large and temporary increase of cosmic-ray intensity which occurred on February 23, 1956, in association with a solar flare. During the period of enhanced intensity a balloon-borne neutron detector measured the absorption mean free path and intensity of the flare particles at high altitudes. From these experiments the primary particle intensity spectrum as a function of particle rigidity, over the range <2 to >15–30 Bv rigidity, has been deduced for different times during the period of enhanced intensity. It is shown that the region between the sun and the earth should be free of magnetic fields greater than $\sim 10^{-6}$ gauss and that the incoming radiation was practically isotropic for more than 16 hours following maximum flare particle intensity. The decline of particle intensity as a function of time t depends upon the power law $t^{-3/2}$, except for high-energy particles and late times, where the time dependence approaches an exponential. The experiments lead to a model for the inner solar system which requires a field-free cavity of radius greater than the sun-earth distance enclosed by a continuous barrier region of irregular magnetic fields [B (rms) $\approx 10^{-5}$ gauss] through which the cosmic-ray particles must diffuse to reach interstellar space. This barrier is also invoked to scatter flare particles back into the field-free cavity and to determine the rate of declining intensity observed at the earth. The diffusion mechanism is strongly supported by the fact that the time dependence $t^{-3/2}$ represents a special solution of the diffusion equation under initial and boundary conditions required by experimental evidence. The coefficient of diffusion, the magnitude of the magnetic field regions, the dimensions of the barrier and cavity, and the total kinetic energy of the high-energy solar injected particles have been estimated for this model. Recent studies of interplanetary space indicate that the conditions suggested by the experiments may be established from time to time in the solar system. The extension of the model to the explanation of earlier cosmic-ray flare observations appears to be satisfactory.

The solar flare event was superposed by chance upon a large but typical intensity decrease of nonsolar cosmic rays which began several days prior to February 23. Hence, the flare particles have been used as probes to explore the intensity modulation mechanism responsible for this decrease of background cosmic-ray intensity.

I. INTRODUCTION

THE fifth large increase of cosmic-ray intensity known to occur in association with a solar flare took place on February 23, 1956. This was the largest of all the intensity increases since they were first observed in 1942,[1,2] and it undoubtedly will be the most studied. From these earlier events it was evident that the particles producing the intensity increase occurred predominantly in the low-energy portion of the cosmic-ray spectrum. Therefore, detectors which respond to the secondary radiation from the low-energy portion of the primary cosmic-ray spectrum are of special interest in studying the energy spectrum of flare particles. Over the past eight years a neutron intensity monitor has been developed and used for investigations of this kind at low energies, since more than 0.75 of all cosmic-ray particles to which it is sensitive fall within a magnetic rigidity range where we may use the geomagnetic field as a particle rigidity analyzer. We have established a network of neutron pile monitors to exploit these principles. Locations of the continuous observing stations are shown on the map, Fig. 1. At the time of the flare the sixth neutron monitor, identical with the units at Chicago and Climax, was returning with the U. S. Antarctic Expedition and was operating in the harbor of Wellington, New Zealand. In addition, neutron detection apparatus was carried by a balloon over Chicago during the cosmic ray increase. Thus, the flare of February 23 is of interest since there exists for the first time the means for studying the flare particle intensity as a function of both time and particle rigidity.

We shall report here on the analysis of our experiments and its bearing on the flare particle spectrum, the propagation of the high-energy flare particles in the interplanetary medium, and the relationship of the cosmic-ray event to solar phenomena.

The flare occurred at a fortuitous time in the development of the new solar cycle which began with the minimum in 1954. For a few months preceding the February, 1956 flare, the first intense solar activity got under way with the result that we observed a series of relatively sharp decreases of background cosmic-ray intensity—decreases substantially below the level which was observed at solar minimum. Since we believe these sharp, isotropic decreases to be the result of a modulation effect on the cosmic radiation of nonsolar origin, the superposition of the flare particles upon this reduced cosmic-ray background can be used to limit greatly the possible choices among models for the modulation mechanism acting on the nonsolar radiation.

The main features of the flare particle intensity as a function of both energy and time suggest a description for the magnetic properties of the interplanetary volume centered around the sun and extending out to the order of six astronomical units or more. We shall explore the consequences of this model for forming the solar flare cosmic-ray spectrum, and for astrophysical

* Assisted in part by the Office of Scientific Research and the Geophysics Research Directorate, Air Force Cambridge Research Center, Air Research and Development Command, U. S. Air Force. The laboratory on board the U.S.S. *Arneb* and its operation during the Antarctic Expedition 1955–1956 were supported by funds from the U. S. Committee for the International Geophysical Year.

[1] S. E. Forbush, Phys. Rev. **70**, 771 (1946).
[2] A. Ehmert, Z. Naturforsch. **3a**, 264 (1948).

questions, such as the presence of a galactic magnetic field in the vicinity of the solar system.

Many of the effects reported for the earlier flare events find an explanation in the model we propose. Indeed, the sharp increases of intensity to large values outside impact zones, the arrival of flare particles for hours after all solar activity had ceased, the delayed arrival of the first flare particles for some regions of the earth, and other features are accounted for by this model.

II. OPTICAL, RADIO, AND OTHER OBSERVATIONS OF THE FLARE

Electromagnetic radiation from the sun was directly observable in Asia and Australia at the time of the flare. Although the flare was first observed in progress at 0334 U.T. (Universal Time), its onset was probably near 0331. In Table I we have listed some of the more important flare and flare-related observations made available to us either by private communications or from recently issued publications; hence these data are to be considered provisional.

Of special interest are the radio burst observations since it is well established that the maximum elevation of the radio source in the corona at the time of emission may be determined from a knowledge of the lowest frequencies that reach the earth. Since the coronal electron density decreases with increasing height above the photosphere and the index of refraction must be real for radio waves to escape the corona, then the lowest observable frequency in a radio burst decreases with increasing coronal height. The lowest frequencies

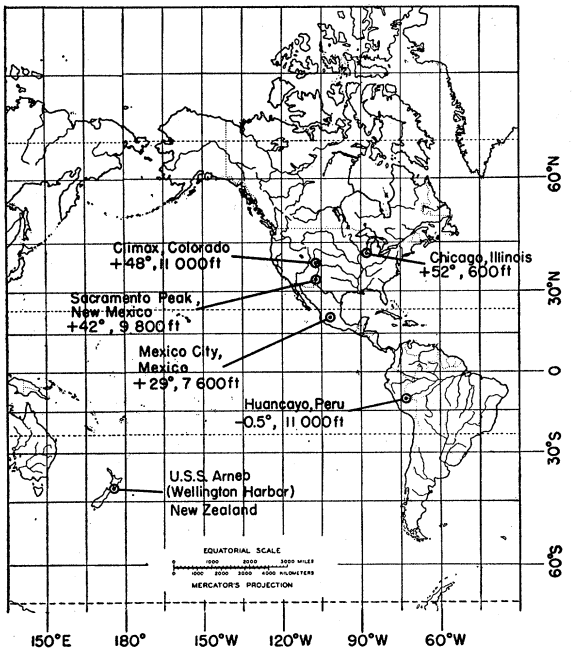

FIG. 1. The locations of the University of Chicago neutron monitor stations operating during the solar flare of February 23, 1956.

TABLE I. Partial list of solar flare and related observations.

Type of observation		Reference
1. Position	74°W; 23°N	a
2. Visual (including H_α)		
(a) first observed	0334 U.T., February 23	a,b
(b) extrapolated beginning	0331 U.T.	a
(c) maximum intensity	0342 U.T.	a,b
(d) H_α line width at 0342 U.T.	18 A	a
(e) area	1.3×10^{-3} of visible hemisphere	a
(f) last observation (not end of visible flare)	0414 U.T.	a
3. Effect on ionosphere		
(a) S.I.D. beginning daylight side of earth	0330 to 0332 U.T.	c,a
(b) Dark side of earth	Effect similar to sunrise on the ionosphere	d
4. Solar radio burst emission		
(a) onset 3000 Mc/sec	0333 U.T.	a
(b) onset 200 Mc/sec	0335 U.T.	a
(c) onset 85.5 Mc/sec	0335 U.T.	c
(d) onset 19.6 Mc/sec	0335 U.T.	c
5. Geomagnetic storm		
Sudden commencement	0309 U.T. February 25	
Horizontal component change	$>270\times10^{-5}$ gauss	e

[a] M. Notuki, Tokyo Astronomical Observatory, Tokyo, Japan (private communication).
[b] A. K. Das, Kodiakanal Observatory, India.
[c] See reference 3.
[d] A. Shapley, C. R. P. L., National Bureau of Standards (private communication).
[e] U. S. Coast and Geodetic Survey, Department of Commerce, Cheltenham Observatory.

were observed at Sydney[3] although the apparatus in use at the time was not directly observing the sun. For the burst to appear at 19 Mc/sec the radio event associated with this flare must have reached a height in the corona of at least 6×10^5 kilometers, or about a solar radius above the photosphere. Clearly this solar event is not restricted to the vicinity of the chromosphere and lower corona, and we shall consider this problem later when we discuss the total energy in the flare.

III. COSMIC-RADIATION OBSERVATIONS

A. Continuous Observations with Neutron Monitors

To measure changes in primary cosmic-ray intensity during the flare we record the intensity of the secondary, nucleonic component generated by the primary radiation. The nucleonic component intensity is indirectly measured by the amount of local neutron production within a pile structure of lead and paraffin. Details on the detector and instrumentation have been described elsewhere.[4] Since we know the response of the neutron detector for the normal cosmic-ray spectrum as a function of geomagnetic latitude and atmospheric depth, we may extrapolate changes of observed intensity to the top of the atmosphere. In this way we deduce the changes in primary intensity.

The map, Fig. 1, shows how our neutron intensity monitors have been distributed since 1951 to take

[3] R. G. Giovanelli (private communication).
[4] Simpson, Fonger, and Treiman, Phys. Rev. **90**, 934 (1953).

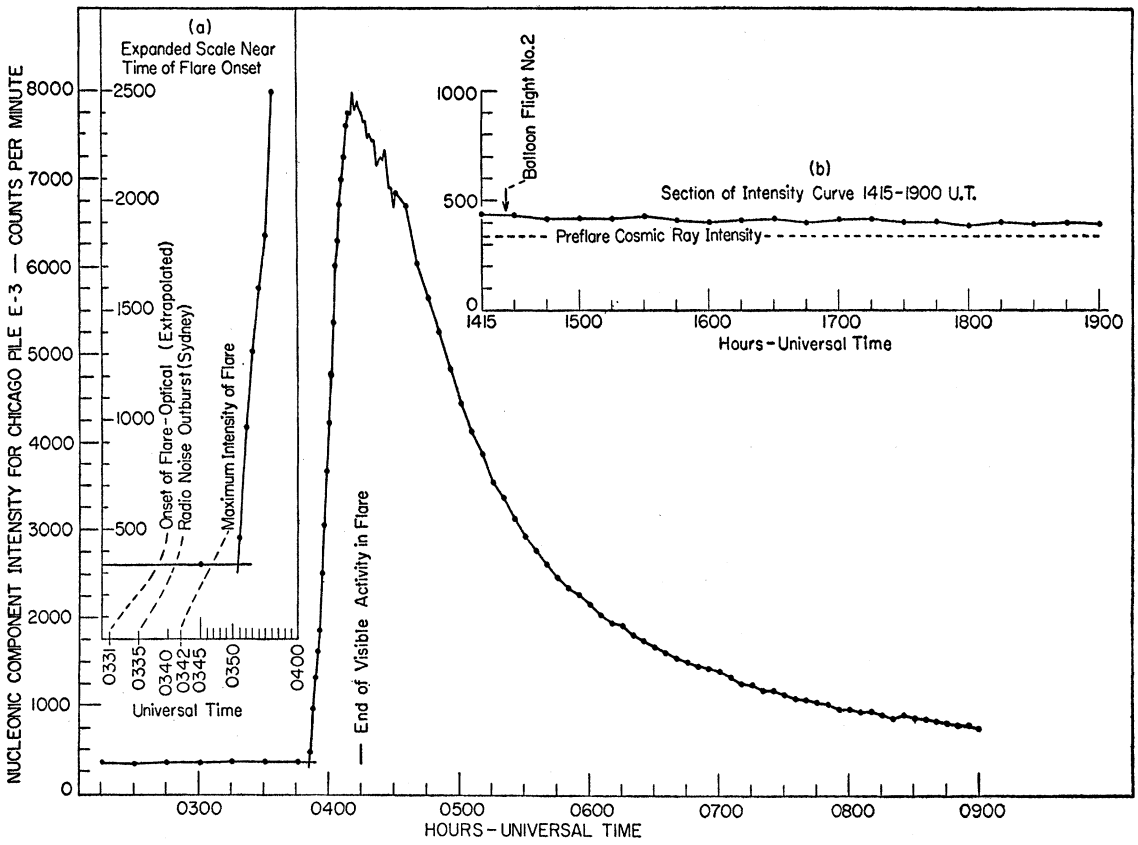

FIG. 2. Nucleonic component intensity as a function of time for the Chicago neutron monitor *E*-3. One-minute intervals are shown between ~0350 and ~0423 U.T. (a) Onset of intensity increase on expanded scale. (b) Period of the cosmic ray increase during which balloon flight number 2 was undertaken (see also Fig. 5).

advantage of a wide range of geomagnetic cutoff rigidities. At the time of the flare an additional monitor was operated on board the U.S.S. *Arneb* in Wellington Harbor, on its return voyage from the U. S. Antarctic Expedition 1955–1956.

Both the stations at Chicago and on the U.S.S. *Arneb* were equipped with special alarm systems which change the recording intervals from 15 minutes to one minute intervals as soon as the intensity rises approximately 60% above normal. The other stations record at time intervals as follows: Mexico, 15 minutes; Climax, 20 minutes; Sacramento Peak and Huancayo, 30 minutes.

The neutron intensity as a function of time outside of impact zones is shown in Fig. 2 for Chicago, and in Fig. 3 for Wellington Harbor. These two widely separated stations yield precise information on the time of onset, the rate of rise, the maximum intensity and the rate of decline of the temporary increase. In Fig. 4 we display the intensity at all six stations as a function of time.

The data from these curves will enable us to obtain information on the flare particle rigidity spectrum at different times during the progress of the event.

B. High-Altitude Observations with Balloons

The warning from the flare alarm system at Chicago made it possible to prepare and launch a balloon flight which reached an altitude of approximately 90 000 feet during the time of the intensity increase. We detected neutrons of moderate energy produced in the air by the nucleonic component with apparatus which included a BF_3 proportional counter surrounded with 2.5-cm paraffin, a precision pressure indicator, and a telemetering system to record the information in the laboratory. From the curve for the neutron intensity as a function of altitude we obtain the absorption mean free path of the nucleonic component in the atmosphere. For high altitudes a neutron intensity maximum exists where the atmospheric depth is approximately equal to the diffusion mean free path of the neutrons. This maximum, which occurs at about 60 mm Hg shown in Fig. 5, makes it possible to compare changes of total primary cosmic-ray intensity among different balloon flights. Over the past three years we have flown this type of equipment to study primary intensity variations.

To measure the mean free path of the nucleonic component produced by the flare particles, we must also

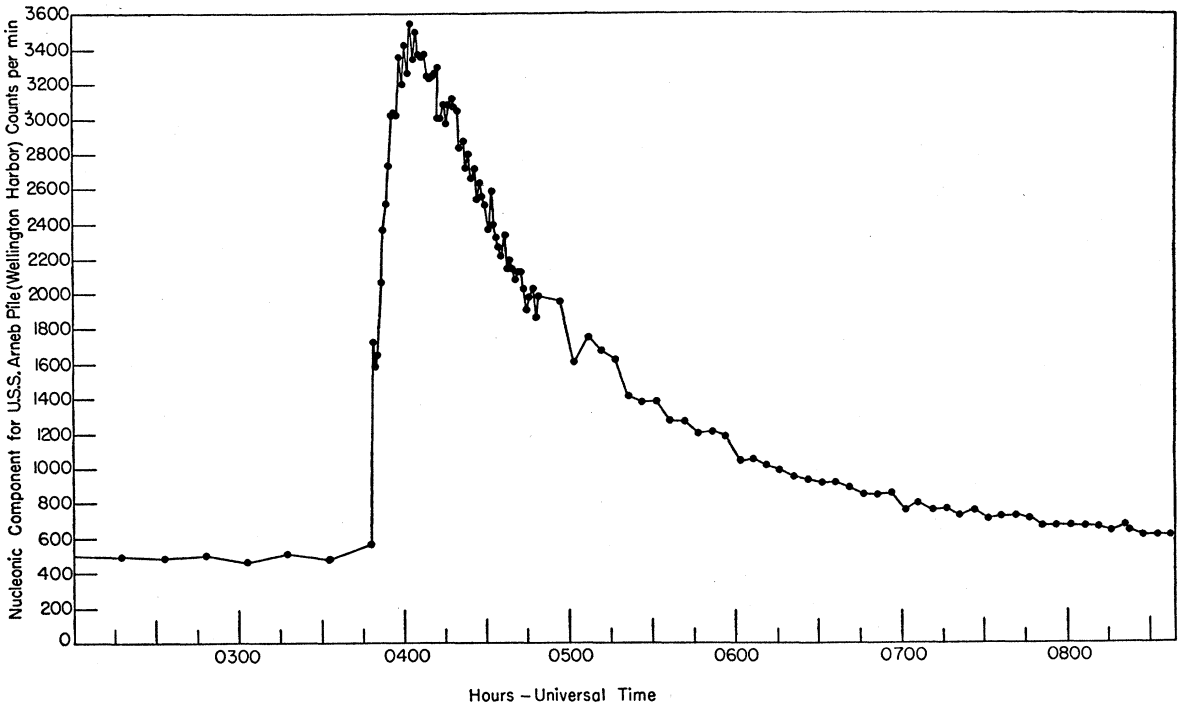

FIG. 3. Nucleonic component intensity as a function of time for neutron monitor A-2 located on board the U.S.S. *Arneb* anchored in Wellington Harbor, New Zealand at the time of the flare. One-minute intervals are shown between 0348 and 0445 U.T. The change in rate of rise of intensity appears to be real.

know the mean free path of the cosmic-ray background prevailing at that time. Since the total cosmic-ray intensity declined sharply several days before the event, we have used the results of our balloon flight of February 18, 1956 (flight number 1) to represent the intensity-altitude distribution of the background radiation at the time of the flare, Fig. 5. Flight number 2 reached maximum altitude at about 1430 U.T. on February 23. At the neutron intensity maximum the intensity was 180% above normal cosmic-ray intensity, whereas the sea-level detector at Chicago was 28% above normal at the same time. To obtain an independent estimate of the flare particle spectrum at the time of flight number 2, we shall later determine this greater attenuation of the nucleonic component arising from the flare particles.

IV. RESULTS OF THE COSMIC-RAY NEUTRON MEASUREMENTS

A. Conclusions

Before undertaking an analysis of the flare particle spectrum, we wish to point out several conclusions which may be drawn from the experimental data as they have been presented in Figs. 2–5. They are:

(1) The temporary increase of cosmic-ray intensity represents the acceleration of particles to cosmic-ray energies in the vicinity of the sun. No hypothesis of focusing, particle storage at the sun, or terrestrial phenomena can account for this enormous increase of cosmic-ray intensity.

(2) The incident cosmic radiation which produces the "tail" of the intensity curve at low energies probably represents particles coming to the earth from many directions in the solar system. This conclusion is supported by the evidence that the radiation continues to arrive for more than 15 hours after all indications of

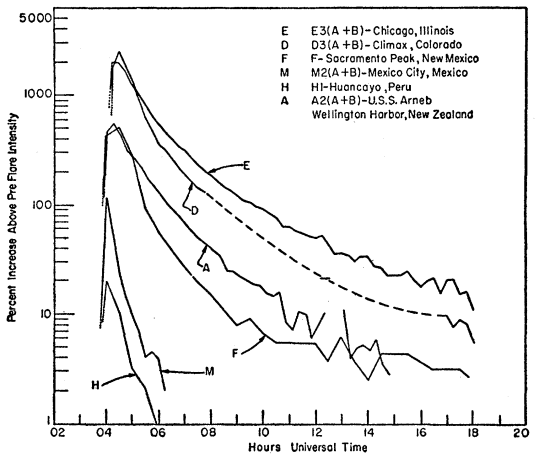

FIG. 4. The percent increase of nucleonic component intensity above background as a function of time for all University of Chicago neutron monitor stations in operation at the time of the solar flare of February 23, 1956. (See Fig. 1 for locations of the stations.)

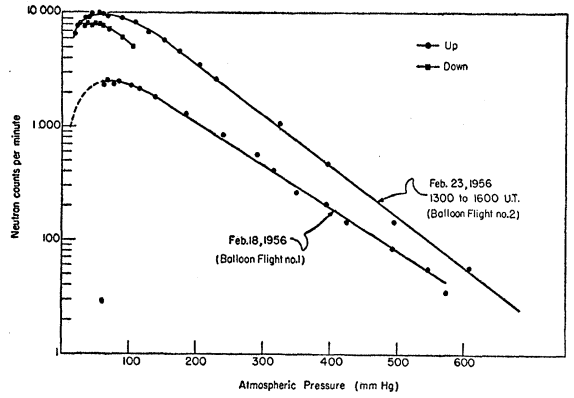

FIG. 5. The cosmic-ray neutron intensity as a function of altitude: balloon flight No. 1 five days preceding the flare. Balloon flight No. 2 occurred during the period of enhanced intensity on February 23 as shown in Fig. 2.

activity in the solar region have disappeared. The lack of intensity increases superposed on the flare intensity curves for Chicago, Climax, and Sacramento Peak, near 0400 and 0900 local time impact zones, is further strong evidence that the particles at those times were not coming directly from a "point" source in the direction of the sun.

(3) To preserve the sharp increases of cosmic-ray intensity after onset as shown in Figs. 2 and 3, the particles must have traversed relatively uncomplicated orbits—hence it is unlikely that scattering regions necessary to account for the "tail" could lie inside the orbit of the earth. Since at onset both Chicago and Wellington were in nonimpact zones, the anomalously large scale of the effect measured there could reasonably be accounted for by requiring that the particles arrive more or less isotropically. Hence, although the orbits are not complicated they must involve at least some scattering, with the scatterer located outside the orbit of the earth. This requires that no appreciable magnetic fields lie between the sun and the earth at the time of the flare.

(4) Particles with energies in excess of 15 Bev, and probably 20–30 Bev, were produced at the time of the flare. We derive this result from the relatively large increase of intensity at the geomagnetic equator (Huancayo, Peru) where the minimum energy for arrival of protons from the vertical is 15 Bev.

B. Flare Particle Spectrum

There are two assumptions underlying our analysis of the flare-particle spectrum. First, we restrict our analysis to the period following the intensity maximum where we believe that the incoming radiation has become isotropic. From this assumption it then follows that we may use Störmer theory in determining the geomagnetic cutoff as a function of latitude for the flare particles. Second, we assume that the composition of the incoming radiation is not significantly different from the composition of the normal cosmic radiation. Primary neutrons as the main component are excluded since the flare increase was observed at full intensity on the night side of the earth. The problem then reduces to whether electrons, protons, or alpha particles constitute the principal flare radiation. Though electrons may possibly be abundant in the primary flare spectrum, their contributions to the secondary nucleonic component can be estimated to be less than 1%, assuming that they are just as abundant in the primary radiation as the protons.

The contribution of alpha particles or heavier nuclei to the primary flare intensity is a more difficult problem. From earlier work we know that both the alpha particle and proton specific yields for neutrons produced in our detectors show roughly similar dependencies on energy per nucleon (within a small constant factor), and at low energies (<4 Bev) the specific yields fall off rapidly with decreasing energy.[4] But for a given particle rigidity, an alpha particle has a smaller per-nucleon energy than a proton. Hence, with increasing geomagnetic latitude λ the proton primaries become increasingly more important than the alpha particles in contributing to the neutron latitude effect for the cosmic-ray flare increase. In fact, for magnetic cutoff rigidities corresponding to $\lambda \gtrsim 45°$ the nucleonic component latitude dependence of the temporary intensity increase reflects only the changes in the proton spectrum. We conclude that by far the greatest contribution to the flare increases observed at Chicago (52°), Climax (48°), and Wellington (−45°) arises from a primary proton component in the flare particle spectrum. We shall return later to the question of the composition and its influence on the form of the primary spectrum.

Using the above assumptions, we construct the primary spectrum for the flare particles at any time after approximately the first hour of flare onset in the following way. For each of the 6 monitor stations, the vertical geomagnetic cutoff is given and the fractional increase at each monitor above normal intensity (Figs. 2–5) yields the relative intensity for flare particles above each geomagnetic cutoff. We have to extrapolate the observed fractional increase for each monitor from deep within the atmosphere to the top of the atmosphere, but we already know that the spectrum is much steeper than the normal spectrum and the integral flare particle intensity above a given geomagnetic cutoff is, therefore, not greatly different from the differential intensity in the vicinity of that cutoff rigidity. Since the absorption mean free path for the normal nucleonic component for all geomagnetic latitudes has been measured,[5] we may use these mean free path data to determine the nucleonic component mean free path for each narrow rigidity range of primary flare particles just above each monitor cutoff rigidity.

To convert the relative increases at the top of the

[5] J. A. Simpson, Phys. Rev. **83**, 1175 (1951).

atmosphere to a spectrum we take the normal, integral cosmic-ray spectrum in the range 2–20 Bv rigidity as proportional to $N^{-1.3}$, where $N=pc/Ze$ is the magnetic rigidity for the vertically incident particles.

Following these procedures we obtain the spectrum for vertically incident flare particles at 0500, 0900, and 1400 hours U.T., as shown in Fig. 6. The spectra at these different times are roughly similar in spite of the fact that the intensity has dropped by more than an order of magnitude. The spectra follow approximately the power law N^{-7}, although there is evidence that the intensity for high-rigidity particles tends to decrease more rapidly with time than the intensity for low rigidities.

We pointed out earlier that protons produced the intensity increases at high geomagnetic latitudes. If the proportion of alpha particles, either completely or partially stripped, is greatly in excess of that for the normal spectrum, then the increases observed at high geomagnetic cutoffs (Mexico and Huancayo) would be partly due to alpha particles. Thus, the magnitude of the exponent for the approximate power law spectra derived from Fig. 6 is the lower limit for the true primary particle spectrum.

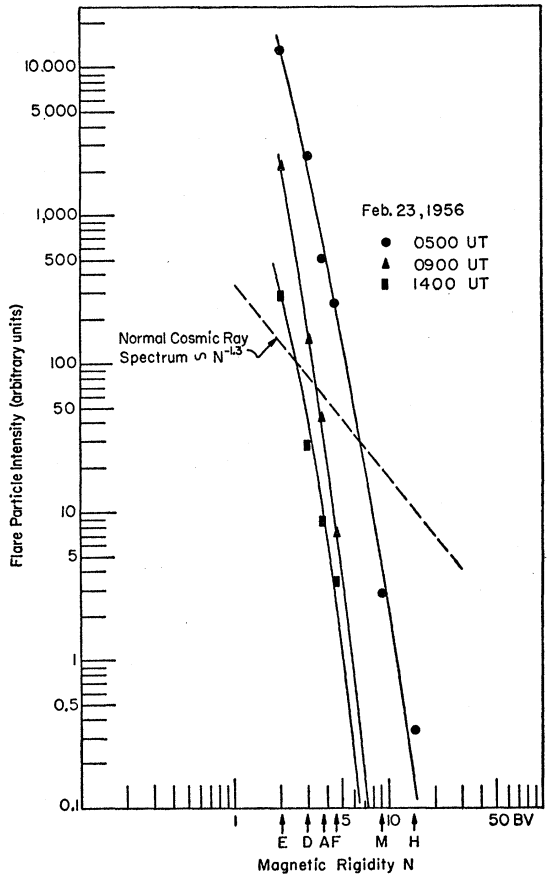

FIG. 6. The integral rigidity spectrum of the primary particles from the solar flare for different times during the period of enhanced intensity. These spectra are derived from the nucleonic component data.

We obtain independent evidence for the character of the flare-particle spectrum at low particle rigidities from balloon flights number 1 and 2. From Fig. 5 we obtain 120 g/cm² for the absorption mean free path of the nucleonic component produced by the primary flare particles alone. To find the range of rigidities for these primary particles, we again use the absorption mean free path measurements for the normal cosmic radiation obtained with detectors having the same response as our balloon borne neutron equipment.[5] We find that 120 g/cm² corresponds approximately to the absorption mean free path for the normal primary radiation lying in the vertical cutoff rigidity range 2 to 4 Bv.[5] Since we have assumed, on the basis of evidence stated earlier, that the radiation after ~0500 hr arrives practically isotropically, we conclude that at the time of flight number 2 the primary spectrum was strongly peaked at particle rigidities just above the geomagnetic cutoff rigidity at Chicago.

From Fig. 6 we note that over 95% of all the particles in the flare spectrum derived from monitor data lie within the rigidity range 2–4 Bv, in agreement with these independent balloon flight observations.

C. Time Dependent Properties of the Cosmic-Ray Intensity

Our discussion of the results has so far been limited to the construction of the primary flare rigidity spectrum at discrete times after the incoming radiation has become essentially isotropic. We now consider the behavior of flare intensity for different particle rigidities as a function of time. We also wish to investigate the time for onset and maximum intensity for detectors both inside and outside impact zones.

From Fig. 4 it is clear that the declining intensity, particularly for the lower rigidity primaries, cannot be represented by an exponential function of time. To search for a possible power law dependence on time, the data in Fig. 4 have been plotted on the log-log scale, Fig. 7. We shall later show that the very good fit of the low-rigidity data with a power dependence on time t, $t^{-3/2}$ in particular, is important for our understanding of the propagation of the flare particles in the interplanetary medium. We find that this power law requires diffusion of the initially produced flare particles out of the solar system. We note that at high energies, or for later times at low energies, the power law breaks down.

Since we have indicated that inside the earth's orbit there is negligible scattering, we have invoked diffusion beyond the orbit of the earth. An independent check on this deduction is obtained from the study of the times at which the flare particles can first arrive in impact zones and in nonimpact zones, namely, the onset times. Both Chicago and Wellington are on opposite

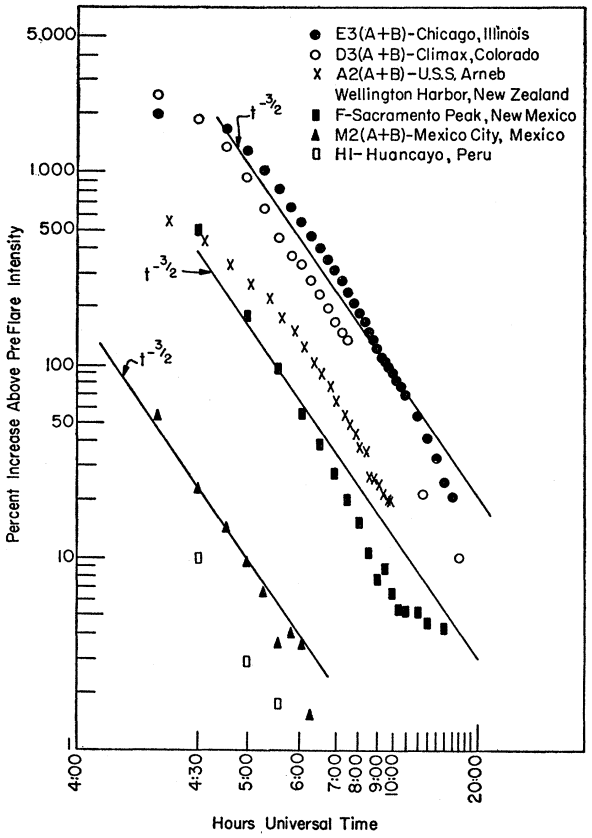

FIG. 7. The percent increase of the nucleonic component intensity as a function of time t plotted on log-log coordinates. The lines of constant slope represent a function proportional to $t^{-3/2}$ with the initial condition that $t=0$ at 0350 U.T.

hemispheres and not in impact zones, although the observed intensities were anomalously large. The onset time at Chicago, Fig. 2, is $0350_{-1.0}{}^{+0.5}$ U.T. in close agreement with 0348±1 U.T. for Wellington, Fig. 3. In contrast with this, we know that the equator station is accessible to cosmic-ray orbits that connect directly with the sun.† Forbush[6] has kindly supplied us with the onset time at Huancayo for the shielded ion chamber located near our neutron monitor. For these high-energy particles, the onset is 0345±1 U.T. and within an impact zone at higher latitude this early onset time is also well established—see, for example, Sittkus *et al.*[7] Thus, a real onset time difference of ~5 minutes between particles that may reach the earth directly and particles arriving outside of impact zones appears to exist. The effect cannot be interpreted in terms of either (a) the lower energy particles arriving later than the high-energy particles along orbits connecting the sun and earth, or (b) the lower energies being produced later at the sun since, for example, the flare increase observed at Leeds with a neutron monitor displayed the early onset time <0345, but was inside the 0400 impact zone.[8] Consequently, the answer must lie in the shorter path lengths for the particles arriving in impact zones over those arriving outside of impact zones.

Sittkus *et al.*[7] have suggested that this difference in onset time arises from some reflecting region beyond the orbit of the earth. In this way the particles arriving at regions outside of impact zones will have undergone scattering. This could explain the delay in onset time for detectors outside of impact zones.

The radius of closest approach for this scattering region to the sun can be estimated from the difference in onset times, and has the value of 1.2 to 1.4 astronomical units (A.U.). As we pointed out earlier, since the rise time of the flare event is very short, the interplanetary volume lying within ~1.4 A.U. radius of the sun is remarkably free of regions which could scatter particles of cosmic-ray energy and the "reflectivity" of the scatterer must be high.

These ideas are consistent with the observed differences in rise time of the particle intensity between stations in impact and nonimpact zones. Estimates from the Leeds[8] and Freiburg[7] data indicate that the time to reach maximum intensity, t_m, was ~8 minutes in the 0400 hour impact zone; whereas, for Chicago t_m was greater by more than a factor of two.

In addition to the differences in the value of t_m inside and out of impact zones, t_m decreases with increasing flare particle rigidity as shown in Table II.

V. A MODEL FOR THE COSMIC-RAY EVENT

We now direct our attention to the explanation of the cosmic-ray flare effect. It is clear from the experiments that there are several physical conditions within the solar system which must be satisfied in order to explain the observations on February 23, 1956. These conditions may be summarized as follows:

TABLE II. Variation of t_m with flare particle rigidity.

Magnetic latitude	Detector	Time of onset U.T.	Time of onset Local	Time of maximum intensity U. T.	t_m min
t_m for detectors outside principal impact zones					
52°	Neutron	$0350_{-1.0}{}^{+0.5}$	2150	0408	18
48°	Neutron	0348	2048	0410	
−45°	Neutron	0348±1	1548	0402	14
45°	Neutron	0348	2048	0400	12
29°	Neutron	0345−50	2145	0400	<15
t_m for detectors inside impact zones or on direct sun-earth orbits[c]					
56°	Neutron[a]	0345	0345	<0400	~8
0°	Ion chamber[b]	0345±1	2245	0400	<15

[a] See reference 8.
[b] See reference 6.
[c] See †.

† R. Lüst in our laboratory has shown that for a source width of ⩾15° there are orbits connecting the source with Huancayo.

[6] S. E. Forbush (private communication), and J. Geophys. Research **61**, 155 (1956).

[7] Sittkus, Kuhn, and Andrich, Z. Naturforsch. **11a**, 325 (1956); Z. Naturforsch. (to be published).

[8] Marsden, Berry, Fieldhouse, and Wilson, J. Atm. and Terrest. Phys. (to be published).

(1) There exists a magnetic field-free region extending outward past the orbit of the earth to approximately $r \approx 1.4$ A.U.

(2) There is a boundary region which scatters cosmic-ray particles back into the field-free region.

(3) Since the particle intensity declines only slowly after reaching maximum intensity, the boundary region must be a barrier for the escape of particles from the field-free region.

(4) The decline of intensity follows a power law $t^{-3/2}$ and not an exponential function of time. Consequently, the barrier is continuous around the field-free region, and is not thin.

(5) It then follows that the field-free region is a volume surrounded by a barrier of finite thickness for the escape of cosmic-ray particles into the galaxy.

This description of the interplanetary volume derived from experiment suggests that the cosmic-ray flare particles diffuse through the barrier from the field-free region. If we let $J(E)dE$ represent the density of cosmic-ray particles with energies in the range $(E, E+dE)$, then we shall assume that $J(E)$ varies according to the diffusion equation

$$\partial J(E)/\partial t = \kappa(E)\nabla^2 J(E), \tag{1}$$

where $\kappa(E)$ is the diffusion coefficient for particles of energy E. We find that there is a solution to the diffusion equation which may have the same $t^{-3/2}$ dependence on time which we found from experiment, Fig. 7; namely,

$$J(E) = \frac{C}{(\pi\kappa t)^{\frac{3}{2}}} \exp(-r^2/\pi\kappa t). \tag{2}$$

Equation (2) is the special solution of Eq. (1) where a burst of radiation is instantaneously released at $t=0$ and at the origin ($r=0$) of an infinitely extensive diffusing medium. This is a problem well known in the theory of heat conduction. If we observe the change in particle density near the source (small values of r), then $J(E) \propto 1/t^{3/2}$ for all energies.[9]

Obviously, this is an oversimplification of the physical conditions, if for no other reason than that we know the diffusing region has an inner boundary at $r \sim 1.4$ A.U. and does not exist for $0 \leq r \leq 1.4$ A.U. Therefore, for simplicity in developing a model we shall assume that the field-free region is a spherical cavity of radius $a = 1.4$ A.U. From Fig. 7 we also know that the function

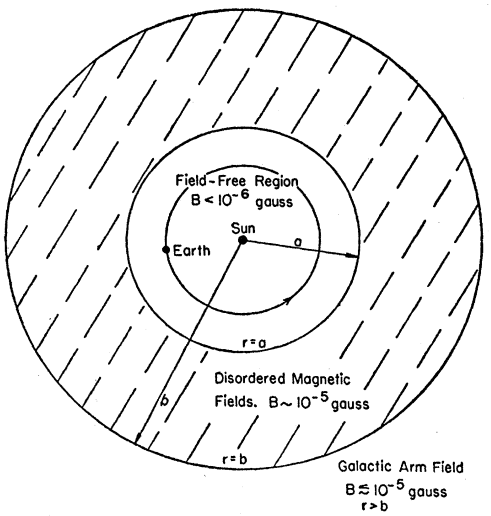

FIG. 8. Cross section of the model for the inner solar system at the time of the solar flare of February 23, 1956. The inner volume $r=a$ represents a cavity "free" of magnetic fields (B (rms) $<10^{-6}$ gauss). The barrier of thickness $b-a$ represents the shell-like region through which the cosmic rays diffuse.

$t^{-3/2}$ does not hold at high energies and, for later times, even at low particle energies. This indicates, as we shall later show, that the diffusing medium is not infinite in extent. For a barrier of finite thickness we shall assume the outer boundary is spherical and at radius b in order to preserve a simple model. These simplifying assumptions lead us to the picture shown in Fig. 8 for the cross section of the inner solar system.

Although the model proposed here rests upon the experimental data from the February 1956 flare, it is important to note that the requirement for a field-free region $r > 1.0$ A.U. in extent, a scattering region and a delay in the eventual escape of the flare particles from the solar system were already deduced from the earlier flare events.[10] Hence, we hope that the hypothesis proposed here may be extended to all flare particle observations.

A. Properties of the Interplanetary Medium

Before treating this idealized model more rigorously let us review the known properties of interplanetary space to decide whether the special conditions proposed here may, in fact, exist. Observations of zodiacal light[11] indicate that the electron density in interplanetary space decreases outward from the solar corona to the order of 400–600 electrons/cm^3 at the orbit of the earth, this density being supported by observations of radio wave whistlers.[12] For these low densities the gas is completely ionized with a kinetic temperature

[9] We wish to point out that for a wide range of primary particle energies, the intensity of secondary radiation measured deep in the atmosphere should also display the $t^{-3/2}$ dependence. During the interval of time when the $t^{-3/2}$ dependence appears to be valid, only particles with energy in excess of the geomagnetic cutoff energy E_c arrive at the atmosphere. If $G(E)$ represents the number of counts per unit of time produced in the detector by one primary particle/cm^3 of energy E, the detector counting rate is

$$R = \int_{E_c}^{\infty} G(E)J(E; r_c, t)dE = \frac{1}{t^{3/2}} \int_{E_c}^{\infty} G(E)J(E; r \approx 0)dE,$$

which varies rigorously as $t^{-3/2}$ for all values of E_c. No other solution of the diffusion equation has this simple property.

[10] J. A. Simpson, Proceedings of the Vth International Cosmic Radiation Conference, Guanajuato, Mexico (1955) (unpublished); Proc. Natl. Acad. Sci. U. S. (to be published).

[11] A. Behr and H. Siedentopf, Z. Astrophys. **32**, 19 (1953).

[12] L. R. O. Storey, Trans. Roy. Soc. (London) **A246**, 113 (1954).

T of the order of thousands of degrees. Chapman[13] has recently calculated that the temperature at the orbit of the earth may be $\sim 10^5$°K. Consequently, the electrical conductivity of the interplanetary medium is high, being given approximately by

$$\sigma = 2\times 10^{-14} T^{3/2} \text{ emu}$$

for ionized hydrogen,[14] while the medium in bulk is electrically neutral.

There is strong evidence that this ionized gas is of solar origin and we now believe that this gas, in the process of escaping from the sun, will occasionally transport away from the sun small amounts of the general solar magnetic fields.[15,16] Additional gas in the form of clouds and so-called solar streams may escape field-free.

If there were no outward moving gas we would expect that the galactic arm magnetic field, estimated by Chandrasekhar and Fermi[17] to be the order of 10^{-5} gauss, would penetrate all interplanetary space. However, as suggested by Davis,[18] the diverging, ionized emission of gas encounters the lateral pressure $B^2/8\pi$ of the galactic magnetic field and will "push" the field outward until this lateral pressure is in equilibrium with the momentum flux of the escaping ionized gas. Thus, a field-free cavity is formed which encloses at least the inner solar system.

For simplicity we have assumed that this cavity has roughly spherical form. At the cavity boundary there must be some form of transition region where irregularities are produced in the otherwise smooth galactic arm field by the irregular gas pressures and gas clouds containing their own magnetic fields. The question of how high-energy charged particles behave in passing through magnetic field irregularities has been studied by Morrison[19] and Parker.[20] The irregularities act as "scattering" centers for the charged particles. Given the magnetic field intensity in these local regions, along with their concentration, the effective diffusion mean free path for a charged particle of energy E can be determined. Thus, the boundary region produces scattering and slow diffusion of the cosmic-ray particles, while, at the same time, defining a roughly spherical volume of radius r containing no general magnetic field with rms field density $>10^{-6}$ gauss, and where r has the value $r>1.0$ A.U. at the time of the cosmic-ray increase.

[13] S. Chapman, Monthly Notices Roy. Astron. Soc. (to be published).
[14] T. G. Cowling, *The Sun* (University of Chicago Press, Chicago, 1953).
[15] If the escaping "cloud" of conducting gas is of scale length l, the magnetic field permeating the cloud will decay in a time the order of $l^2\sigma$. For example, if l is 10^{-2} A.U. (1 A.U. $=1.5\times 10^{13}$ cm =sun-earth distance) then $l^2\sigma \approx 3\times 10^6$ years for $T=4000$°K.
[16] H. W. Babcock and H. D. Babcock, Astrophys. J. **121**, 349 (1955).
[17] S. Chandrasekhar and E. Fermi, Astrophys. J. **118**, 113, 116 (1953).
[18] L. Davis, Phys. Rev. **100**, 1440 (1955).
[19] P. Morrison, Phys. Rev. **101**, 1397 (1956).
[20] E. N. Parker, Phys. Rev. **103**, 1518 (1956).

B. Special Solutions for the Model

With these concepts in mind, we now explore in more detail the hypothesis of a field-free cavity surrounded by an irregular magnetic field barrier region, Fig. 8. Within the barrier $J(E)$ varies according to Eq. (1). We know from elementary kinetic theory that the diffusion coefficient $\kappa(E)=\frac{1}{3}cL(E)$ for relativistic particles with a mean free path $L(E)$.

To develop the model more completely, we review and extend the simplifying assumptions:

(1) The diffusion barrier possesses spherical symmetry about the sun with the inner surface of the barrier at radius $r=a$ and the outer surface at $r=b$.

(2) The diffusing region extends uniformly from $r=a$ to $r=b$ so that $\partial\kappa(E)/\partial r=0$ within the barrier.

(3) At the time $t\leq 0$ the particle density outside the cavity is zero, and at the instant $t=0\equiv t_0$ the cavity is uniformly filled to a density $J_0(E)$. This neglects the transit times for particles in the cavity. Similarly, the diffusion equation (1) neglects transit times in the barrier.

The solution of Eq. (1) is worked out in Appendix A with these assumptions, and we shall consider here three special cases of interest.

Case I.—Assume that $b^2\gg a^2$. Since the quantity $(\pi^2\kappa t)^{\frac{1}{2}}$ is a measure of the distance beyond r to which the particles have diffused in time t, then for $r\gg(\pi^2\kappa t)^{\frac{1}{2}}$ we know that $J(E;r,t)$ does not differ significantly from zero and we sum Eq. (16A) only over the values of $r\leq(\pi^2\kappa t)^{\frac{1}{2}}$.

If t is selected so that $a^2\ll\pi^2\kappa t\ll b^2$, we may replace the discrete summation in Eq. (16A) by an integration over n, so that

$$J(E;r,t)\sim\frac{\pi}{6}J_0(E)\frac{a^3}{(\pi\kappa t)^{\frac{3}{2}}}\exp\left(-\frac{r^2}{4\kappa t}\right), \qquad (3)$$

and the decay of intensity observed at the earth ($r\cong 0$) varies as $t^{-3/2}$.

Case II.—Assume that $b\gg a$ and t is of such a value that $\pi^2\kappa t\gtrsim b^2$. We then find from Appendix A, Eqs. (16A) and (18A) that the series converges rapidly because of the exponential term, and near the cavity where $r\ll b$, we have

$$J(E;r,t)\sim\tfrac{2}{3}\pi^2 J_0(E)\left(\frac{a}{b}\right)^3\exp\left(-\frac{\pi^2\kappa t}{b^2}\right)\{1+\cdots\}. \qquad (4)$$

Case III.—Assume that the barrier is thin, namely, $(b-a)\ll a$. Then we obtain from Eqs. (14A) and (15A)

$$J(E;r,t)=J_0(E)\frac{b-r}{b-a}\exp\left[-\frac{3\kappa t}{a(b-a)}\right], \qquad (5)$$

and the decay of cosmic-ray intensity at the earth is exponential for all values of t.

The experimental evidence from Figs. 4 and 7 shows that the decay of intensity with time is not exponential

but follows a $t^{-3/2}$ power law. Hence we must assume that $b \gg a$ as in Case I. By the time t' the particles have diffused into the thick barrier a distance the order of a, so $\pi^2 \kappa t' \approx a^2$, the particle density inside the cavity begins to decrease as $t^{-3/2}$, as given by Eq. (3) and in agreement with Fig. 7. The particle density continues to decrease as $t^{-3/2}$ until particles begin to emerge from the distant outer surface of the barrier at $r=b$, at which time $\pi^2 \kappa t \approx b^2$, and then escape into the more regular and smooth galactic arm field. Then the continuing decrease of intensity observed within the cavity will become exponential as given by (4). We interpret the deviation of the experimental data from $t^{-3/2}$ for later times in Fig. 7 as the onset of the exponential decay, and we shall later use this evidence to estimate the value for b on February 23, 1956.

The energy dependence of the diffusion coefficient becomes important at high energies. We have $\kappa(E) = \frac{1}{3} c L(E)$, and if we assume that L is of the same order of magnitude as the Larmor radius of the particles in the barrier magnetic field regions, then

$$L(E) \approx \frac{E_0 [\xi(\xi+2)]^{\frac{1}{2}}}{ZeB},$$

where E_0 is the rest energy, $\xi = E/E_0$, Ze is the charge on the particle in esu, and B is the field intensity in gauss. Thus, we see that $\kappa(E)$ is approximately proportional to E for particle energies of several Bev or more.

We note from Table II that the higher energy particles reached maximum intensity and also, from Fig. 7, began to decline as $t^{-3/2}$ earlier than the very low-energy particles. Both these effects may be understood from the fact that the diffusion coefficient $\kappa(E)$ increases with increasing particle energy. During the total period of time that the flare region ejecting particles into the field-free cavity, (the order of 20–30 minutes on the basis of our model), the high-energy particle density rapidly reached equilibrium, with the particles leaking out through the barrier as rapidly as they were produced by the flare. Hence, the high-energy particle density began to decrease almost as soon as their rate of production by the flare region began to decline, whereas the particle density of low-energy particles, leaking out of the barrier only relatively slowly, continued to rise for nearly as long as the flare region could produce them. Thus, the effective time $t=0$ for reaching equilibrium is determined by $\pi^2 \kappa t \approx a^2$, and therefore, the decline of intensity should be written as a function of $(t-t_0)^{-3/2}$, where t_0 occurs earlier for high-energy particles than for low-energy particles, as shown by the experimental data, Table II.

We summarize the two ways in which the primary intensity as a function of time will depart from $t^{-3/2}$ for our model. First, the barrier thickness is finite and the flare particles may begin to escape from the outer regions of the barrier before the intensity at the earth has returned to normal. This effect would appear late in the decline of the flare particle intensity. Second, for particles of high energy the diffusion constant increases so that the "effective" barrier depth is small, as for Case III. We expect and find both of these effects, Fig. 7.

C. Influence of Cosmic-Ray Background Intensity

The data in Fig. 7 are obtained by subtracting the normal cosmic-ray background from the total intensity; hence, the choice of interpolated background intensity influences the shape of the curves at low flare particle intensity and at late times in two ways. First, when the intensity is only slightly above normal a small error in background introduces a large error in the flare particle intensity. Second, at high energies (low-latitude stations) the intensity variations in cosmic-ray background are smaller than for low energies (high-latitude stations). Hence, even small flare-intensity increases at high energy (e.g., Huancayo) may be measured accurately. The background intensities for the curves in Figs. 4 and 7 are obtained by interpolating between pre- and post-flare intensity for each station.

D. Barrier Dimensions and the Coefficient of Diffusion

From arguments in Sec. IV C we note that $a \approx 1.4$ A.U. We may estimate b from the observed deviation of the intensity from $t^{-3/2}$ for large values of t; for example, about 6–8 hours after the onsets at Chicago and Climax the counting rates were declining faster than $t^{-3/2}$. Hence, we assume that after about 8 hours, $\pi^2 \kappa t$ was comparable to b^2. The intensity dependence on time was going over into an exponential decay, at which time the intensities had declined by a factor ~ 50 suggesting that

$$(4/3)\pi b^3 \approx 50 \times (4/3)\pi a^3,$$

from which we conclude that $b \approx 5$ A.U. Since b depends upon the $\frac{1}{3}$ power of the intensity, this is a fairly precise estimate.

There are two independent estimates for the value of $\kappa(E)$. First, the flare particle intensity began to fall off as $t^{-3/2}$ for low-energy particles (2–4 Bev) about one hour after onset, implying that $\pi^2 \kappa t \approx a^2$. With $a \approx 1.4$ A.U., this yields $\kappa(2\text{–}4 \text{ Bev}) \approx 1.1 \times 10^{22}$ cm^2/sec. Second, we noted that after ~ 8 hours $\pi^2 \kappa t$ was becoming comparable to b^2. This yields $\kappa(2\text{–}4 \text{ Bev}) \approx 0.7 \times 10^{22}$ cm^2/sec with the value of b already estimated.

E. Barrier Magnetic Field Intensity

Since $\kappa = \frac{1}{3} c L$, we conclude that $L > 10^{12}$ cm for $\kappa \approx 10^{22}$ cm^2/sec. If we assume that L is the same order of magnitude as the radius of curvature of the particles in the disordered barrier field, then the rms field intensity in the barrier has an upper limit $B < 2 \times 10^{-5}$

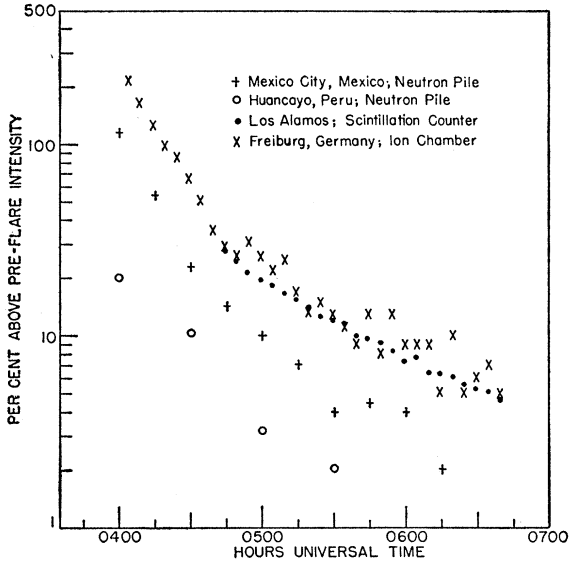

FIG. 9. The percent increase of cosmic-ray intensity as a function of time for detectors that respond to primary particles of energy ≥ 10 Bev—on a semilog plot. The Mexico and Huancayo neutron data are obtained from Fig. 4. The detector at Los Alamos was a 600-liter scintillation counter.[21] See reference 11 for the Freiburg data.

gauss which happens to be comparable to the galactic arm field of $\sim 6\times 10^{-6}$ gauss.[17]

F. Exponential Decay

It has been pointed out earlier that at high particle energies the intensity decline should approximate an exponential as for Cases II and III. To investigate the energies for which this effect sets in, we have compared the neutron intensity data from our Mexico ($E>10$ Bev) and Huancayo monitor ($E>15$ Bev) with the observations obtained from a large liquid scintillator (~ 600 liters) at Los Alamos, New Mexico.[21] This detector has a very high counting rate and responds to primary particles of energy $E>8$–10 Bev. The results are shown in Fig. 9, and indicate that there is evidence for exponential decay at energies as low as the order of 10 Bev beginning about an hour after the onset of the intensity increase.

G. Other Neutron Data for February 23, 1956

In Fig. 10 we have plotted the neutron intensity data from several other observers[8,22–25] both inside and out of impact zones for low and intermediate primary particle cutoff energies. It appears that the intensity decreases as $t^{-3/2}$ for several hours with deviations from this dependence at later times. These results are similar to the observations from our neutron monitor network.

VI. COSMIC-RAY INCREASE OF NOVEMBER 19, 1949

Among the four earlier large cosmic-ray intensity increases the most data exist for the flare of November 19, 1949.[26] At that time a neutron detector at Manchester observed an increase of factor 5 with a subsequent intensity decline extending for more than 12 hours.[27] This neutron detector at $\lambda \approx 57°$N measured the effect of low-energy primary particles, but the decline of intensity followed an approximate exponential function of time in contrast with our observations for the February, 1956 flare. To show how this observation may be accounted for with the model we propose, we shall consider Case III, Sec. V, for which $(b-a)\ll a$ to obtain exponential decay.

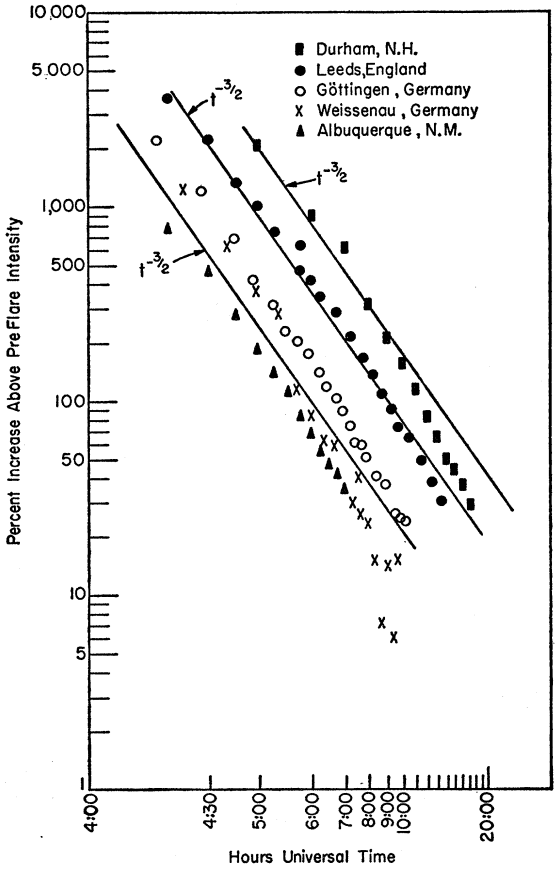

FIG. 10. The percent increase of the nucleonic component intensity as a function of time on log-log coordinates. The lines of constant slope represent a function proportional to $t^{-3/2}$ with the initial condition that $t=0$ at 0350 U.T. The measurements are reported from Durham, New Hampshire[22]; Leeds, England[8]; Gottingen, Germany[23]; Weissenau, Germany[24]; and Albuquerque, New Mexico.[25]

[21] E. C. Anderson, Los Alamos Scientific Laboratory. We wish to thank Dr. Anderson and the U. S. Atomic Energy Commission for permission to use the liquid scintillator counter data.

[22] Lockwood, Yingst, Calawa, and Sarmaniote, Phys. Rev. **103**, 247 (1956).

[23] B. Meyer, Z. Naturforsch. **11a**, 326 (1956).

[24] A. Ehmert and G. Pfotzer, Z. Naturforsch. **11a**, 322 (1956).

[25] R. R. Brown (private communication).

[26] H. Elliot, *Progress in Cosmic-Ray Physics* (North Holland Publishing Company, Amsterdam, 1952). Forbush, Stinchcomb, and Schein, Phys. Rev. **79**, 501 (1950).

[27] N. Adams, Phil. Mag. **41**, 508 (1950). N. Adams and H. J. J. Braddick, Phil. Mag. **41**, 505 (1950).

This condition leads to two possible sets of values for the parameters a and b at the time of the 1949 event.

(1) b may have been very small. This appears rather unlikely in view of the intense solar activity underway during the year preceding the flare.

(2) a may have been large. This is more likely since we suspect the total output of solar gas had recently passed its maximum, and the solar field-free cavity would be near its greatest extension.

The second alternative is further supported by the fact that the delays in the magnitude of onset times and t_m between impact and nonimpact zones was greater than for the 1956 event.

Other features of the 1949 and earlier flares have already been postulated[10] to require a field-free region >1 A.U. and an extended scattering region, in agreement with the cavity-barrier model.

VII. SUPERPOSITION OF FLARE PARTICLES ON A COSMIC-RAY MODULATION EFFECT

In view of the severe restrictions we have placed upon magnetic fields and scattering within the solar cavity at the time of the flare, it is especially important to understand the origin of the isotropic and rapid decrease of cosmic-ray intensity (Forbush-type decrease) which began $\sim$10 days prior to the flare event and continued beyond the period of the flare (see Fig. 11). In recent years experiments have shown that this isotropic decrease is not of terrestrial origin, and hence, the mechanism producing it must lie outside the geomagnetic field. Experiments have also shown that the magnitude of this phenomenon is a function of particle rigidity and is a modulation of the pre-existent cosmic radiation by a solar controlled mechanism.[28]

We have discussed elsewhere the possibility for distinguishing among the several hypotheses of cosmic-ray modulation by studying the superposition of the flare particle spectrum on the modulated pre-existent cosmic rays[29]; we treat the flare particles as probes for studying electromagnetic conditions in interplanetary space.

The experimental evidence cited above supports modulation by magnetized and ionized clouds. The question then arises: How is it possible for these cloud-like regions to expand outward from the sun carrying their tangled magnetic fields without introducing such serious scattering within $\sim$1 A.U. that the observed features of the cosmic-ray flare event would be destroyed? The magnetic field intensity and scale length of the model clouds proposed by Morrison[19] to account for a rapid intensity decrease and continuing low intensity level ($\sim$10% decrease at Climax) are more than an order of magnitude too large to permit observation of the flare event. An alternative explanation,[20] where in the magnetized cloud is captured by the earth and is supported outside the geomagnetic field, namely, a geocentric cloud, does not meet with these objections. For the geocentric model we find that with scattering and diffusion limited to regions near the earth, there is negligible effect on the flare particle orbits.

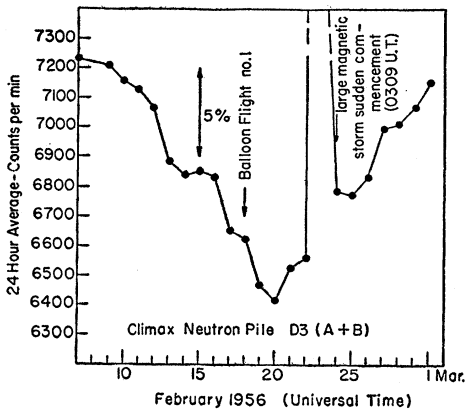

FIG. 11. The daily average nucleonic component intensity for neutron monitor D-3 at Climax, Colorado. The isotropic decrease of intensity for cosmic rays of nonsolar origin has superposed upon it the solar injected flare particles of 23 February 1956.

VIII. CONSEQUENCES OF THE FLARE OBSERVATIONS AND SOLAR CAVITY MODEL

A. Total Energy of Flare Particles

We may estimate the total kinetic energy of the cosmic-ray particles produced by the flare of February 23, since at the time t_m of maximum intensity, we believe that substantially all of the low-energy particles were still within the solar cavity. For this estimate we shall assume that all of the particles are protons distributed isotropically in the cavity by time t_m. The energy spectrum of flare particles decreases so rapidly with increasing energy that to good approximation we may neglect the contribution of all particle energies above the geomagnetic cutoff of the neutron monitor at Sacramento Peak ($\sim$5 Bev) and consider only the intensity increase in the interval between Sacramento Peak and Climax ($\sim$3 Bev) as representing the total contribution of flare particles above $\sim$3 Bev. Hence, most of the increased counting rate at Climax arose from primary particles in the energy interval 3–5 Bev; the ratio for the factor of increase at Climax over Sacramento Peak, namely 25/5, supports this conclusion.

Under normal circumstances the cosmic radiation in the energy range 3–5 Bev contributes 4×10^{-4} erg cm^{-2} sec^{-1} sterad^{-1} at the top of the atmosphere, yielding an energy density of 1.7×10^{-13} erg/cm^3 in interplanetary space. These particles account for approximately 0.1 of the total counting rate at Climax on the basis of aircraft measurements of the neutron latitude effect at the atmospheric depths of Sacramento Peak and Climax.[30] The counting rate at Climax was

[28] J. A. Simpson, Phys. Rev. **94**, 426 (1954).
[29] J. A. Simpson, Ann. géophys. **2**, 305 (1955).
[30] P. Meyer and J. A. Simpson, Phys. Rev. **99**, 1517 (1955).

25 times the cosmic-ray background rate at t_m and, therefore, 250 times the normal counting rate arising from primary particles in the range of 3–5 Bev. Hence, the intensity of 3–5 Bev particles actually increased by the factor 250, and their particle energy density was 4×10^{-11} erg/cm^3 within the cavity. If this is the density at time t_m throughout the cavity of radius 1.4 A.U., then the total energy for flare particles of energy in excess of 3 Bev is 1.4×10^{30} ergs.

To this must be added the total energy of particles <3 Bev. Even if there is a low-energy spectrum cutoff which varies with the solar cycle, our knowledge of atmospheric absorption and other effects leads to an estimate of not less than a factor 2–3 for the additional contribution of lower energy particles. We thus obtain a lower limit of $\sim3\times10^{30}$ ergs for the kinetic energy in flare produced cosmic-ray particles.

Since this total energy for flare particles of cosmic-ray energy is greatly in excess of the energy estimated to be released in the form of other radiations, the possibility exists that there are large amounts of energy still unobserved in the electromagnetic radiation from a flare. Possibly the total energy going into x-radiation has been greatly underestimated.

From the model we deduce that the total time for particle emission was t_m; hence the average power output from the flare in the form of cosmic radiation was $\sim1.5\times10^{27}$ ergs/second.

In Sec. II we noted that this solar flare was unusual in the sense that its radio emission originated as far out as a solar radius from the photosphere. This evidence, along with the estimates of the total energy output from the flare region, lead us to suspect that the optical flare effect was a minor part of the total solar process.

B. Production Spectrum of Flare Particles

In Fig. 6 we have derived from experimental data the primary particle spectrum observed for $t>t_m$ in the vicinity of the earth. The model we have proposed to explain the time dependence of the flare particle intensity requires that the high-energy particles diffuse out of the "field-free" cavity in less time than the low-energy particles. Hence, after t_m the particle spectrum is steeper than at the time of solar production; namely, if we may represent both the production spectrum and cavity spectrum by a power function N^{-n}, then, since $n\approx7$ for the cavity spectrum, $n<7$ for the solar production spectrum.

C. Solar Flares on the "Back-Side" of the Sun

Since the model proposed for the temporary storage of flare cosmic-ray particles requires isotropy and roughly uniform particle density throughout the field-free region of the inner solar system, we would expect that the cavity could be filled equally well by particle injection from a flare on the invisible portion of the sun. Obviously, no impact zones could exist at the earth, but we should observe a slow rise in intensity followed by a gradual decline to normal background intensity.

If the solar flare of February 23 had occurred on the invisible portion of the sun, we would have expected a lower total intensity, but comparable in magnitude to the high-latitude neutron monitor observations on February 23.

No outstanding event of this type has been reported. Since neutron monitor observations are most suitable for these measurements, we can only examine the past 6-year period. In that time only 1–2 solar flare events on the visible disk would have been expected to produce a large cosmic-ray increase. Hence, it is rather likely that no similar event has occurred on the invisible solar disk during these past six years. Also, for flares occurring at times when the field cavity is very large (such as we suspect was the case for November 19, 1949) the observed intensity increase would indeed be small.

IX. CONCLUDING REMARKS

Without invoking a model or theory for the injection and propagation of solar flare cosmic-ray particles, we conclude from our experiments that:

(1) In association with a solar flare the sun injects particles of cosmic-ray energy into interplanetary space.

(2) The interplanetary volume extending from the sun to beyond the earth is free of magnetic fields with rms intensity $B\gtrsim10^{-6}$ gauss.

(3) After reaching maximum intensity, the particles arrive from practically all directions in the sky, isotropy prevails during the decline of intensity.

(4) The decline of intensity is a function of time t such that $\mathcal{J}(E)\propto1/t^{3/2}$ for low-energy primary particles and for several hours during the decline. For high-energy particles the intensity approaches an exponential function of time.

(5) Solar-produced particles continue to arrive at the earth for more than 15 hours after all evidence of associated solar activity has ceased.

(6) The integral intensity $\mathcal{J}'$ of primary particles as a function of particle rigidity pc/Ze is given by $\mathcal{J}'\propto[pc/Ze]^{-7}$ which holds for several hours following maximum intensity. At high rigidities the spectrum tends to fall off more steeply with particle rigidity.

(7) Primary protons account for the major part of the intensity increases observed at geomagnetic latitudes $\lambda\gtrsim45°$. Primary neutrons could not produce the observed effects with our detectors. Alpha particles may be present, but it appears unlikely they could be the principal component in the primary cosmic-ray flux.

(8) Primary particles having rigidities <2 Bv to >15–30 Bv contribute to the primary spectrum.

(9) No large scale distribution of interplanetary magnetic fields can be invoked to account for the sharp and extensive decreases of cosmic-ray intensity for particles of nonsolar origin. The use of flare-injected cosmic-ray particles acts as a probe for testing different

hypotheses for intensity modulation of pre-existant cosmic rays.

From our experiments we are then led to the following requirements for a suitable model:

(1) The particles do not escape into interstellar space in straight lines, but are stored for a period the order of hours in the vicinity of the sun.

(2) The particles undergo scattering beyond the orbit of the earth, producing remarkable isotropy of the radiation.[31] The isotropy is achieved by the time the flare particle intensity has passed its maximum.

(3) Since the particles are delayed in their escape from the solar system, the region which produces the backscattering is most likely also the barrier for the escaping radiation.

(4) With the intensity decline following a $t^{-3/2}$ dependence on time, diffusion is the most likely mechanism for escape through the barrier since a solution of the classical diffusion equation gives $\mathcal{J}(E) \propto t^{-3/2}$ with reasonable initial and boundary conditions.

(5) The entire field-free volume must be enclosed by the barrier for the solution of the diffusion equation to hold. Thus, for simplicity the model requires a field-free volume of radius >1 A.U. (radius ≈ 1.4 A.U. from the additional data of Forbush and Sittkus).

(6) Under the above conditions, the total time for injection at the sun may be 20 to 30 minutes or less. For the time scale of the entire event, this simulates instantaneous injection of the flare particles into the cavity.

From these general deductions we have constructed a specific model which appears to account for even some of the more subtle points in the experiment. We estimated the size of the barrier, the diffusion coefficient, the barrier field intensity, and other essential parameters from the experimental data.

We have discussed the main properties of interplanetary space which indicate that this hypothesis may have a physical foundation. It appears that gas clouds carrying tangled magnetic fields may exist and attempt to escape radially from the solar system. These, and other highly ionized field-free clouds of gas may sweep back any ordered solar or galactic magnetic fields which would otherwise prevade the entire interplanetary space. We have assumed that the barrier is represented by these tangled fields piled-up over a region forming a shell with inner radius 1–2 A.U. We do not know the degree of stability of such a barrier against penetration by ordered fields, but we do know from simple hydromagnetic concepts that the time constants are the order of months, or more. For our purposes it is sufficient to point out, as we did in the Introduction, that the flare event was preceeded by months of intense solar activity which should be capable of forming the special conditions required for the barrier region.

The model appears to account for the main features of the earlier flare events, and, indeed, a study[10] of the early flare events (particularly November 19, 1949) had already established the deductions 1, 2, 3, and 6.

Several additional large intensity increases from solar particle injection in the future will be required before the generality of the model proposed here can be adequately tested.

Although the network of six neutron monitor stations and balloon-launching facilities are part of our research facility at the Institute, their successful operation rests in large measure upon assistants in the field. We wish at this time to express our deep appreciation to the many individuals who have assisted at the following stations: At Huancayo, Peru, Mr. Herman Goller and Mr. Albert Giesecke, Jr., with the cooperation of the Government of Peru have made it possible to establish excellent observing conditions. At Mexico City, Professor Sandoval Vallarta and the University of Mexico have generously made facilities available, and Dr. Jose y Coronado has supervised the station operation. The Sacramento Peak pile has been operated by Dr. Edward Manring and the staff at the Peak under Dr. John Evans. At Climax, Colorado, our laboratory is under the care of Mr. Richard Hansen and Mr. C. Dodgen, with help of many kinds from Dr. Walter O. Roberts of the High Altitude Observatory. At Chicago the neutron pile has been operated by Mr. Manfred Pyka and Mr. Neil Sullivan.

For the neutron monitor observations on board the U.S.S. *Arneb*, we are grateful to Mr. Rochus Vogt, who kept the apparatus in excellent condition throughout the expedition to the Antarctic.

The laboratory on board the U.S.S. *Arneb* was the result of close cooperation and contributions from the U. S. National Committee for the International Geophysical Year and the U. S. Navy Task Force 43 represented by Admiral George Dufek and his staff.

Assistance with the balloon launching program and special electronic circuits was given by F. Jones, R. Blenz, and R. Weissman.

The reduction and preparation of data for analysis was carried out by Gordon Lentz, James Ayers, Neil Sullivan, and Randolph Shen.

We wish to thank our many colleagues who forwarded to us the results of their observations prior to publication, and, especially, we thank Mr. M. Notuki of the Tokyo Observatory, Dr. R. Giovanelli of Sydney, Australia (Division of Radio Physics) CSIRO, Dr. Das of Kodaikanal, South India, and Mr. Allen Shapley of Radio Propagation Physics Division, National Bureau of Standards.

The data from our neutron station network have been sent to Mr. Thomas Gold, Greenwich Observatory, who is collecting all available data on the solar event of February 23, 1956, for future distribution.

[31] F. Bachelet and A. M. Conforto, Nuovo cimento **3**, 1153 (1956).

APPENDIX A

Consider the diffusion of particles of density $J(E,r,t)$ out through a uniform spherical shell in which the coefficient of diffusion is κ. We let the inner radius of the shell be $r=a$ and the outer radius $r=b$, so that κ is uniform and nonzero only in the interval $a<r<b$. We assume that at time $t=0$ the inner cavity ($r\leq a$) is filled uniformly to a density $J_0(E)$ and no particles have yet diffused into the shell, $r>a$, so that $J(E,r,0)=0$ for $r>a$. We let $J_1(E,t)$ represent the uniform particle density in the cavity $r<a$, so that $J_1(E,0)=J_0(E)$. Since the particle density is a continuous function of r for $t>0$ we have $J_1(E,a,t)=J_1(E,t)$; since the rate of decrease of the total number of particles in the cavity is just equal to the rate of diffusion into the shell at $r=a$, we have

$$\frac{a}{3\kappa}\frac{\partial J(E,a,t)}{\partial t}=\frac{\partial J(E,a,t)}{\partial a}. \tag{1A}$$

The solution of this diffusion problem using the Laplace transform is straightforward and similar problems may be found in the literature.[32] We let

$$J(E,r,t)=u(E,r,t)/r, \tag{2A}$$

so that (1) reduces to

$$\frac{\partial u(E,r,t)}{\partial t}=\kappa\frac{\partial^2 u(E,r,t)}{\partial r^2}, \tag{3A}$$

and (1A) becomes

$$\frac{a}{3\kappa}\frac{\partial u(E,a,t)}{\partial t}=-\frac{u(E,a,t)}{a}+\frac{\partial u(E,a,t)}{\partial a}. \tag{4A}$$

We use capital letters to denote the Laplace transform, so that

$$U(E,r,p)\equiv\int_0^\infty dt\,\exp(-pt)u(E;r,t).$$

Transforming (3A) and (4A), we obtain

$$\partial^2 U/\partial r^2-k^2U=0, \tag{5A}$$

and

$$\frac{a}{3\kappa}[k^2\kappa U(E,a,p)-u(E,a,O)]=-\frac{U(E,a,p)}{a}+\frac{dU(E,a,p)}{da}, \tag{6A}$$

where

$$k^2=p/\kappa. \tag{7A}$$

[32] H. S. Carslaw and J. C. Jaeger, *Conduction of Heat in Solids* (Clarendon Press, Oxford, 1947).

The solution of (5A) is obviously of the form

$$U=A_1\sinh kr+A_2\cosh kr. \tag{8A}$$

The particle density must vanish at $r=b$, because $\kappa=\infty$ for $r>b$, and must satisfy (4A) at $r=a$. We ultimately find that

$$U(E,r,p)=\frac{a^3J_0(E)}{3\kappa}\times\frac{\sinh k(b-r)}{(\frac{1}{3}a^2k^2+1)\sinh k(b-a)+ak\cosh k(b-a)}. \tag{9A}$$

Using the inversion theorem for the Laplace transform, we obtain

$$u(E,r,t)=\frac{1}{2\pi i}\int_{\gamma-i\infty}^{\gamma+i\infty}dz\,\exp(+zt)U(E,r,z). \tag{10A}$$

From (6A), it is readily shown that the only singularities in $U(E,r,z)$ are simple poles along the negative real axis at the points

$$z_n=-\kappa\alpha_n^2,\quad (n=0,1,2,\cdots), \tag{11A}$$

where the α_n are the roots of

$$(\tfrac{1}{3}a^2\alpha^2-1)\sin\alpha(b-a)=a\alpha\cos\alpha(b-a). \tag{12A}$$

It can be shown that the residue R_n of the pole at z_n is

$$2\pi iR_n=-\tfrac{2}{3}a^3J_0(E)\alpha_n^2\exp(-\kappa\alpha_n^2t)\sin\alpha_n(b-r)\times\{(\tfrac{1}{3}a^3\alpha_n^3-ab\alpha_n^2)\sin\alpha_n(b-a)+(b\alpha_n-\tfrac{1}{3}a^2b\alpha_n^3+\tfrac{1}{3}a^3\alpha_n^3)\cos\alpha_n(b-a)\}^{-1}. \tag{13A}$$

Using (12A) to eliminate $\cos\alpha_n(b-a)$, we obtain, finally,

$$j(E,r,t)=\frac{1}{r}u(E,r,t)=\tfrac{2}{3}a^4\frac{J_0(E)}{r}\sum_{n=0}^{\infty}\alpha_n^3\exp(-\kappa\alpha_n^2t)\frac{\sin\alpha_n(b-r)}{\sin\alpha_n(b-a)}\times[\alpha_nb+\tfrac{1}{3}a^2b\alpha_n^3+(1/9)a^4b\alpha_n^5-(1/9)a^5\alpha_n^5]^{-1}, \tag{14A}$$

from Eq. (10A).

The value for $u(E,r,t)$ represents the solution of the diffusion equation in the region $a<r<b$ when $t>0$. For $r<a$, we have that $J_1(E,t)=u(E,a,t)/a$, which represents the particle density observed at the earth inside the field-free cavity.

To demonstrate the time dependence of the cosmic-ray intensity at the earth during the decay following the flare, we consider several special cases. First we suppose

that $b \gg a$. Then (12A) yields

$$\alpha_n b \sim n\pi + \frac{1}{45}\left(\frac{a}{b}n\pi\right)^5 + O\left(\left(\frac{a}{b}n\pi\right)^7\right), \quad (15A)$$

and

$$u(E,r,t) \sim \frac{2\pi a^3 J_0(E)}{3b^2} \sum_{n=0}^{\infty} n\left[1 - \tfrac{1}{6}\left(\frac{a}{b}n\pi\right)^2 + O\left(\left(\frac{a}{b}n\pi\right)^4\right)\right] \exp\left(-\frac{\kappa n^2\pi^2 t}{b^2}\right) \sin\left(\frac{n\pi r}{b}\right). \quad (16A)$$

The approximation is valid so long as $\pi^2\kappa t \gg a^2$.

When $b^2 \gg \pi^2\kappa t^2 \gg ar$, the terms in the summation are either slowly varying functions of n or else negligible, so that the summation in (16A) may be replaced by an integration, giving finally

$$J(E,r,t) \sim \frac{a^3 J_0(E)}{6\sqrt{\pi}} \frac{\exp(-r^2/4\kappa t)}{(\kappa t)^{\frac{3}{2}}}\left[1 + O\left(\frac{a^2 r^2}{\kappa^2 t^2}\right)\right]. \quad (17A)$$

When $\pi^2\kappa t \gtrsim b^2$, then (16A) may be written

$$J(E,r,t) \sim \frac{2\pi^2 a^3 J_0(E)}{3b^3} \exp\left(-\frac{\pi^2\kappa t}{b^2}\right) \times\left\{1 + 4\exp\left(-\frac{3\pi^2\kappa t}{b^2}\right) + 9\exp\left(-\frac{8\pi^2\kappa t}{b^2}\right) + \cdots\right\}. \quad (18A)$$

When $(b-a) \ll a$, we find that from (15A)

$$a\alpha_n \sim \left(\frac{3a}{b-a}\right)^{\frac{1}{2}}\left[1 - \frac{1}{40}\left(\frac{b-a}{a}\right)^2 + \cdots\right].$$

Hence (14A) reduces to

$$J(E,r,t) \sim J_0(E)\left(\frac{b-r}{b-a}\right) \exp\left[-\frac{3\kappa t}{a(b-a)}\right] \times\left[1 + O\left(\left(\frac{b-a}{a}\right)^{\frac{1}{2}}\right)\right]. \quad (19A)$$